

# Histogram analysis of diffusion kurtosis imaging derived maps may distinguish between low and high grade gliomas before surgery

Xi-Xun Qi<sup>1</sup> · Da-Fa Shi<sup>2</sup> · Si-Xie Ren<sup>3</sup> · Su-Ya Zhang<sup>1</sup> · Long Li<sup>4</sup> · Qing-Chang Li<sup>5</sup> · Li-Ming Guan<sup>1</sup> 

Received: 29 June 2017 / Revised: 16 September 2017 / Accepted: 29 September 2017 / Published online: 16 November 2017  
© European Society of Radiology 2017

## Abstract

**Objective** To investigate the value of histogram analysis of diffusion kurtosis imaging (DKI) maps in the evaluation of glioma grading.

**Methods** A total of 39 glioma patients who underwent preoperative magnetic resonance imaging (MRI) were classified into low-grade (13 cases) and high-grade (26 cases) glioma groups. Parametric DKI maps were derived, and histogram metrics between low- and high-grade gliomas were analysed. The optimum diagnostic thresholds of the parameters, area under the receiver operating characteristic curve (AUC), sensitivity, and specificity were achieved using a receiver operating characteristic (ROC).

**Result** Significant differences were observed not only in 12 metrics of histogram DKI parameters ( $P<0.05$ ), but also in mean diffusivity (MD) and mean kurtosis (MK) values, including age as a covariate ( $F=19.127$ ,  $P<0.001$  and  $F=20.894$ ,  $P<0.001$ , respectively), between low- and high-grade gliomas. Mean MK was the best independent predictor of differentiating glioma grades ( $B=18.934$ ,  $22.237$  adjusted for age,  $P<0.05$ ). The partial

correlation coefficient between fractional anisotropy (FA) and kurtosis fractional anisotropy (KFA) was 0.675 ( $P<0.001$ ). The AUC of the mean MK, sensitivity, and specificity were 0.925, 88.5% and 84.6%, respectively.

**Conclusions** DKI parameters can effectively distinguish between low- and high-grade gliomas. Mean MK is the best independent predictor of differentiating glioma grades.

## Key points

- DKI is a new and important method.
- DKI can provide additional information on microstructural architecture.
- Histogram analysis of DKI may be more effective in glioma grading.

**Keywords** Glioma · Magnetic resonance imaging · Diffusion kurtosis imaging · Histogram analysis · Pathological grade

Xi-Xun Qi and Da-Fa Shi are co-first authors.

✉ Li-Ming Guan  
guanlm66@126.com

<sup>1</sup> Department of Radiology, First Affiliated Hospital of China Medical University, Shenyang 110001, China

<sup>2</sup> Department of Radiology, First Affiliated Hospital of Yangtze University, Jingzhou 434000, China

<sup>3</sup> Department of Radiology, Chengdu Second People's Hospital, Chengdu 610000, China

<sup>4</sup> Department of Neurosurgery, First Affiliated Hospital of China Medical University, Shenyang 110001, China

<sup>5</sup> Department of Pathology, First Affiliated Hospital of China Medical University, Shenyang 110001, China

## Abbreviations

|        |  |
|--------|--|
| AD     | axial diffusivity                                      |
| AK     | axial kurtosis   |
| AUC    | area under the receiver operating characteristic curve |
| CBTRUS | Central Brain Tumor Registry of the United States      |
| CNS    | central nervous system                                 |
| DKE    | Diffusion Kurtosis Estimator                           |
| DKI    | diffusion kurtosis imaging                             |
| DTI    | diffusion tensor imaging                               |
| DWI    | diffusion weighted imaging                             |
| FA     | fractional anisotropy                                  |
| FDT    | FMRIB's Diffusion Toolbox                              |
| FWHM   | full width at half maximum                             |
| KFA    | kurtosis fractional anisotropy                         |
| MD     | mean diffusivity                                       |

|     |                            |
|-----|----------------------------|
| MK  | mean kurtosis              |
| MRI | magnetic resonance imaging |
| NPV | negative predictive value  |
| RD  | radial diffusivity         |
| RK  | radial kurtosis            |
| WHO | World Health Organization  |

## Introduction

Cerebral gliomas are the most common type of primary brain tumours, accounting for approximately 28% of all primary brain and central nervous system (CNS) tumours and 80% of malignant tumours, according to statistics from the Central Brain Tumor Registry of the United States (CBTRUS) [1]. These tumours can be classified into four grades according to the World Health Organization (WHO) based on pathological appearance; grade I-II gliomas are low-grade tumours, while grade III-IV gliomas are high-grade gliomas [2]. Glioma preoperative grading, particularly the differentiation between low- and high-grade gliomas, is of the utmost importance in offering guidance for therapeutic decisions and predicting prognosis [3–6]. Conventional magnetic resonance imaging (MRI) techniques are useful tools in grading gliomas; however, these methods have limited sensitivity and specificity [3, 6, 7].

With the development of MRI techniques, some advanced procedures, such as diffusion-weighted imaging (DWI) [6] and diffusion tensor imaging (DTI) [3, 4, 7], have been widely used in glioma preoperative grading. DWI is a noninvasive *in vivo* imaging technique for the assessment of water molecule diffusive motion in tissues, and this technique can reveal the microstructural architecture of normal and diseased tissues. DTI is an MRI technique based on DWI, and reflects the anisotropic diffusion of water molecules *in vivo* including their orientation and microstructure integrity. The theoretical basis for both DWI and DTI is that the diffusion displacement probability in tissues follows a Gaussian diffusion distribution. However, the complex microscopic environments of tissues; the influence of microstructures and other structures, such as cellular membranes and organelles; the interaction and size of macromolecules; and the tissue viscosity cause the diffusion displacement probability distribution to deviate substantially from a Gaussian form. Thus, DWI and DTI have limitations in accurately reflecting tissue structures and properties.

Diffusion kurtosis imaging (DKI) is an extension of DTI and a new MRI technique that describes the non-Gaussian aspect of water diffusion [8, 9]. DKI enables the use of additional diffusion metrics to estimate microstructural changes and better reflects the microstructural complexity of the examined tissues [5, 8, 10, 11]. DKI provides conventional DTI metrics, such as fractional anisotropy (FA) and mean

diffusivity (MD) and generates particular DKI metrics, including mean kurtosis (MK), kurtosis fractional anisotropy (KFA). Previous studies have demonstrated the utility of DKI for assessing glioma grading [5, 10, 12]. Histogram analysis is a mathematical method that may improve tumour heterogeneity in MRI assessment without additional imaging, and this analysis more comprehensively estimates tumour biological characteristics, including intratumour heterogeneity. Histogram analysis has been widely used in neoplasms for diagnosis, grading, typing, and response evaluation [4, 13–17]. However, the evaluation of glioma grading using DKI histogram analysis has not yet been reported. Hence, the purpose of the present study was to investigate the value of the histogram analysis of DKI-derived maps for the evaluation of glioma grading.

## Materials and Methods

### Patients

Between May 2014 and June 2015, 39 patients who underwent preoperative MRI, including conventional MR (including pre- and post-contrast MR) and DKI, and were pathologically confirmed with gliomas were enrolled in the present study. According to the WHO criteria, among these 39 patients, 13 had low-grade gliomas (seven women and six men, with ages ranging from 31–55 years and a mean age of  $40.08 \pm 8.26$  years), and 26 had high-grade gliomas (11 women and 15 men, with ages ranging from 11–67 years and a mean age of  $54.35 \pm 11.31$  years).

### MRI protocols

All MRI examinations were performed using a 3T MRI system (Verio Syngo; Siemens Medical Solutions, Erlangen, Germany) with an eight-channel head coil. All patients underwent routine pre- and post-contrast MRI and DKI. The imaging protocol included pre-contrast, including axial spin-echo T1-weighted images, fast spine-echo T2-weighted images, fluid-attenuated inversion recovery T2-weighted images, sagittal spin-echo T1-weighted images, DKI, and subsequent contrast-enhanced axial/sagittal/coronal spin-echo T1W images. The DKI dataset was acquired using a spin-echo diffusion-weighted echo-planar imaging sequence in two blocks: a main block with three b values ( $b=0$  s/mm<sup>2</sup>, 1,000 s/mm<sup>2</sup> and 2,000 s/mm<sup>2</sup>) and averages=1 and a secondary block with  $b=0$  s/mm<sup>2</sup> and averages=9 [8, 18]. The other parameters for the two blocks were as follows: TR=6,000 ms, TE=98 ms, field of view=222×222 mm<sup>2</sup>, acquisition matrix=74×74, number of slices=40, slice thickness=3 mm, inter-slice gap=0, and gradient directions=30. The total acquisition times for the two blocks were 6 min 26 s and 1 min 14 s, respectively.

## MRI data processing and histogram analysis

The DKI data were processed using the Diffusion Kurtosis Estimator (DKE) [9] (version 2.6.0, <http://academicdepartments.musc.edu/cbi/dki/dke.html>). Before DKI parameter estimation, we evaluated all the diffusion images to ensure no significant image distortion, and the DKI data were corrected for head motion and eddy current distortions using the “eddy\_correct” tool in FMRIB’s Diffusion Toolbox (FDT) that was listed in the FMRIB Software Library (FSL) (<https://fsl.fmrib.ox.ac.uk/fsl/fslwiki/FSL>). DKE was used for spatial smoothing using a Gaussian filter with a full width at half maximum (FWHM) value of 3.75 mm (an isotropic FWHM approximately 1.25 times the voxel size is recommended by the software) and rigid-body co-registration for the DKI data, and parametric maps were obtained that included the MD, MK, FA, and KFA values estimated by DKE. Based on conventional MR images (pre- and post-contrast) and DK sequence ( $b=0$  s/mm<sup>2</sup>) images, regions of interest (ROIs) were manually drawn on MD maps in slices where in the solid region of the tumours was maximum, and then automatically projected onto the other parametric maps (MK, FA, and KFA maps). Solid portions of the tumours were selected as ROIs, while regions of peritumoural oedema, haemorrhage, cystic change, and necrosis were excluded (Figs. 1 and 2). The ROIs were drawn using Image J software (version 1.51d, National Institutes of Health, Bethesda, MD, USA), and the following parameters were derived from the DKI parameter map histograms: mean, minimum, maximum, median, skewness, and kurtosis.

## Statistical analysis

All statistical analyses were performed using the SPSS statistical package for Windows (version 16.0, Chicago, IL, USA), and all quantitative parameters are reported as  $\bar{x} \pm SD$  and qualitative parameters are reported as frequency and percentage. Univariate linear modelling, including age as a covariate, was used to test differences in metrics in the solid regions between glioma grades, the partial correlation adjusted by age to analyse the dependence of the relationship between FA and KFA in the solid regions of the tumours, and logistical regression was used to identify the best independent predictors of grade among mean DKI parameters adjusted by age. Receiver operating characteristic (ROC) curves were constructed to assess the area under the receiver operating characteristic curve (AUC) and determine the optimum threshold for each histogram metric to differentiate low- and high-grade gliomas. We selected the best Youden index as the best cut-off point.  $P < 0.05$  were considered significant.

## Results

### Comparisons of DKI histogram parameters between low- and high-grade gliomas

Comparisons of DKI histogram parameters adjusted by age between low- and high-grade gliomas are shown in Table 1.

### Correlation between mean FA and mean KFA

The partial correlation coefficient between the mean FA and mean KFA values of the solid portions gliomas, which were adjusted by age, was 0.675 ( $P < 0.001$ ).

### Logistical regression analysis of mean DKI parameters adjusted by age between low- and high-grade gliomas

Logistical regression analysis showed that only the mean MK value was the best independent predictor of differentiating glioma grades (Table 2).

### Evaluation of the diagnostic efficiency of partial DKI metrics histogram parameters in differentiating low- and high-grade gliomas

The ROC analysis showed that mean MD and mean MK could effectively distinguish between low- and high-grade gliomas, particularly MK. The AUC of the mean MK was 0.925, and the sensitivity and specificity were 88.5% and 84.6%, respectively. (Table 3, Fig. 3).

## Discussion

Histogram analysis based on pixel distribution can provide more quantitative information regarding tumour heterogeneity by yielding additional parameters that depict the distribution of signal intensity, such as kurtosis and skewness, both of which can reflect the histogram’s deviation from normal distribution. Histogram analysis of DWI, DTI, and DCE demonstrated their potential for glioma grading [4, 19, 20]. However, to the best of our knowledge, our study was the first to use histogram analysis of DKI to differentiate high- and low-grade gliomas. The results showed that the histogram metrics of MD and MK were significantly different between high- and low-grade gliomas, and the mean MK showed higher values for differentiating high- and low-grade gliomas.

Previous studies have indicated that the apparent diffusion coefficient (ADC) obtained from DWI and the MD obtained from DTI are helpful in the preoperative grading of gliomas. Some studies have reported that the ADC and MD values of high-grade gliomas were significantly lower than those of low-grade gliomas [4, 6, 21]. Xiao et al. [6] and Alexiou

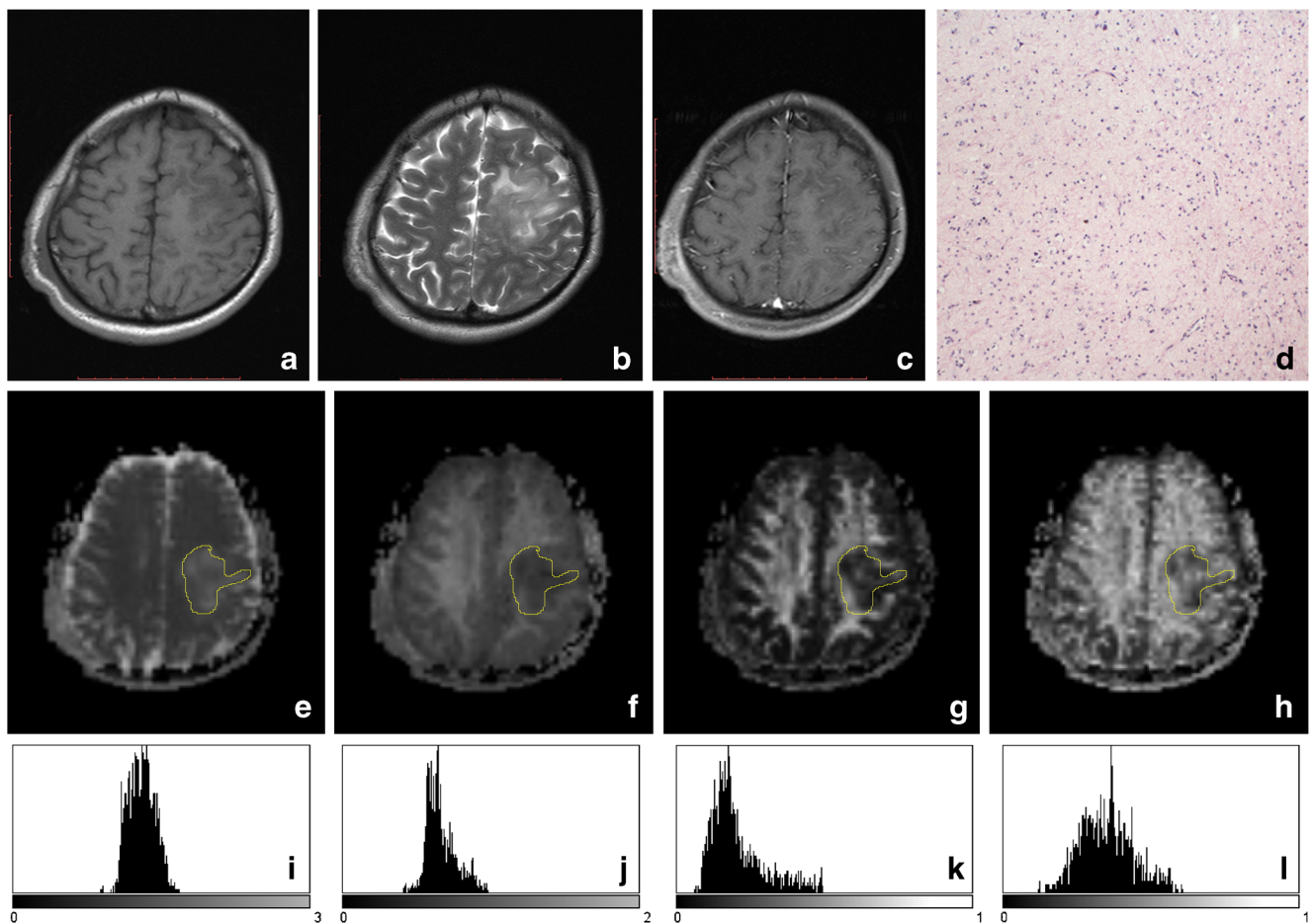


**Fig. 1** A 33-year-old man with astrocytoma (WHO grade II). **a:** The lesion shows low signal intensity on the axial T1-weighted image. **b:** The lesion shows high signal intensity on the axial T2-weighted image. **c:** The lesion shows a slight enhancement effect on axial T1-weighted enhancement imaging. **d:** Pathological analysis confirmed astrocytoma

(WHO grade II) (haematoxylin and eosin,  $\times 200$ ). **e-h:** MD parameter maps, MK parameter maps, FA parameter maps and KFA parameter maps, respectively (the border of the ROI is outlined in yellow on each parameter image). **i-l:** Histograms of the ROIs for MD, MK, FA, and KFA, respectively

et al. [3] showed that the mean 10% ADC value or the relative ADC (rADC) value provided the best differentiation between low- and high-grade astrocytomas. In the present study, the average MD value of low-grade gliomas (1.62) was significantly higher than that of high-grade gliomas (1.23), which was lower than those found in previous studies (1.64 and 1.40, respectively) [21]. These findings likely reflect the pathological characteristics of the gliomas. Cell density and cell composition of gliomas are key factors that determine their pathological grade [3–6, 21]; higher tumour grades exhibit an increased quantity and density of tumour cells; nuclear atypia; and increased polykaryocyte, megakaryocyte and caryoplasm ratios, which restrict the diffusion of water molecules and decrease the ADC/MD values. Tumour grades were reportedly positively correlated with cell density, while ADC values were negatively correlated with cell density and the proportion of nuclei in tumours [22]. However, some studies [7, 23] have shown that no significant difference between the average ADC values of high- and low-grade gliomas exists. This discrepancy may reflect differences in research methods,

scanning parameters, and sample sizes in different studies, and the ADC values may also be affected by glioma vascularity.

In addition, the present study also showed that the minimum, maximum and median MD values of solid regions in low-grade gliomas were significantly higher than those in high-grade gliomas, and the skewness MD values of low-grade gliomas were significantly lower than those of high-grade gliomas. These findings were partially consistent with those of previous studies [6, 23]. Xiao et al. [6] reported that the minimum ADC values of high-grade gliomas were significantly lower than those of low-grade gliomas. Kang et al. [23] also showed that the skewness and kurtosis ADC values in high-grade gliomas were higher than those of low-grade gliomas. These findings provide a more detailed distribution of tumour cells in gliomas. The density and quantity of tumour cells in high-grade gliomas are higher; as a result, the diffusion of water molecules in tumours is more restricted, and the maximum, minimum and median ADC values are all decreased. When the histogram distribution is skewed to the left, the

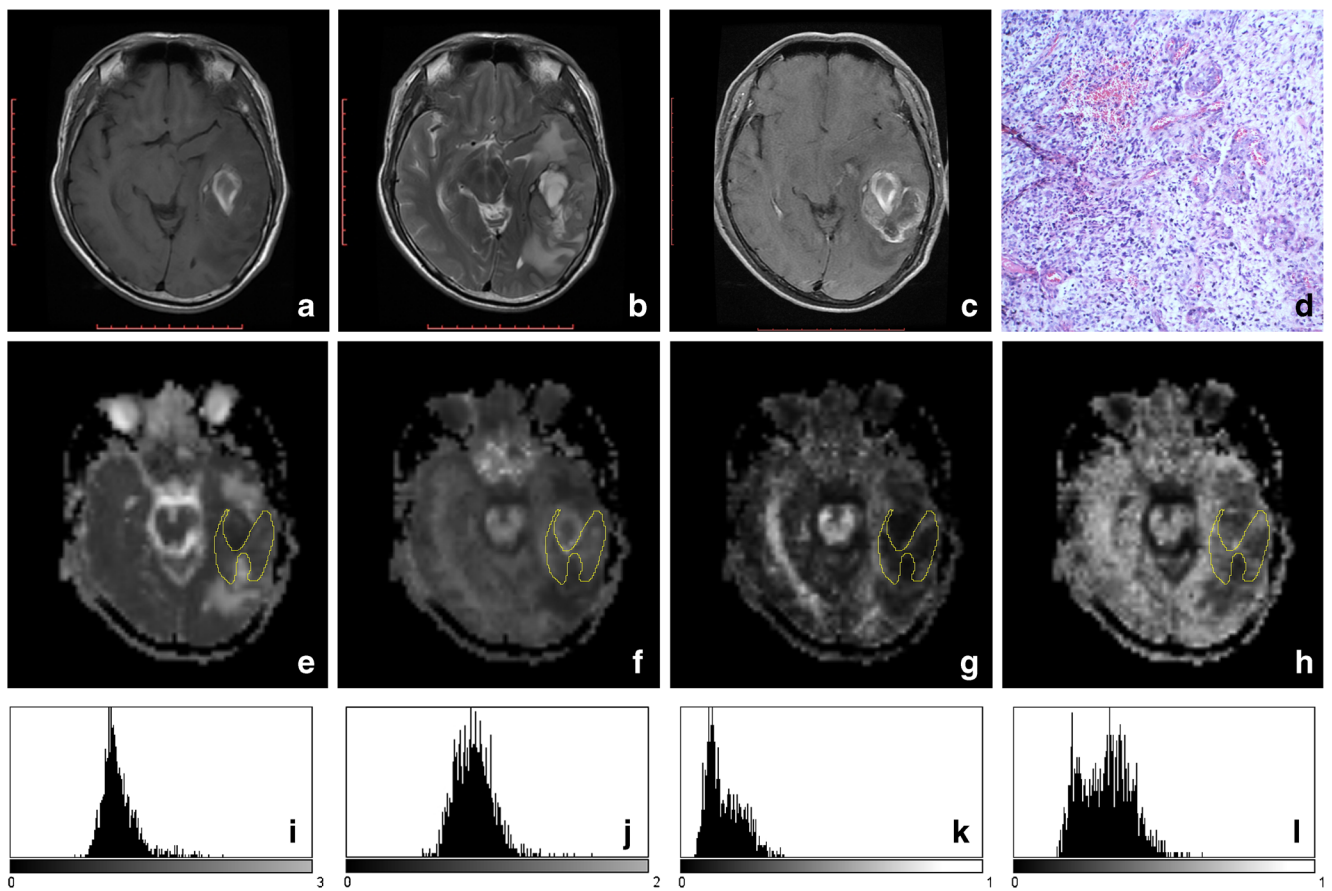


**Fig. 2** A 48-year-old man with glioblastoma (WHO grade IV). **a**: The lesion shows heterogeneous signalling on axial T1-weighted images. **b**: The lesion shows high heterogeneous signalling with a peripheral signal on axial T2-weighted images. **c**: The lesion shows significant inhomogeneous enhancement on axial T1-weighted enhancement imaging. **d**: Pathological analysis confirmed glioblastoma (WHO grade IV)

(haematoxylin and eosin,  $\times 200$ ). **e-h**: MD parameter maps, MK parameter maps, FA parameter maps and KFA parameter maps, respectively (the border of the ROI is outlined in yellow on each parameter image). **i-l**: Histograms of the ROIs for MD, MK, FA, and KFA, respectively

**Table 1** Comparisons of MKI histogram parameters adjusted by age between low- and high-grade gliomas

|     |                | Mean                         | Minimum                      | Maximum                      | Median                       | Skewness         | Kurtosis         |
|-----|----------------|------------------------------|------------------------------|------------------------------|------------------------------|------------------|------------------|
| MD  | Low-grade      | 1.62 $\pm$ 0.32 <sup>a</sup> | 1.11 $\pm$ 0.24 <sup>a</sup> | 2.09 $\pm$ 0.30 <sup>a</sup> | 1.63 $\pm$ 0.35 <sup>a</sup> | -0.12 $\pm$ 0.52 | 0.58 $\pm$ 1.33  |
|     | High-grade     | 1.23 $\pm$ 0.20 <sup>a</sup> | 0.89 $\pm$ 0.18 <sup>a</sup> | 1.85 $\pm$ 0.35 <sup>a</sup> | 1.21 $\pm$ 0.22 <sup>a</sup> | 0.59 $\pm$ 0.77  | 1.05 $\pm$ 2.26  |
|     | <i>F</i> value | 19.127                       | 11.426                       | 6.598                        | 19.095                       | 6.193            | 0.182            |
|     | <i>P</i> value | <0.001**                     | 0.002**                      | 0.015*                       | <0.001**                     | 0.018*           | 0.672            |
| MK  | Low-grade      | 0.49 $\pm$ 0.11              | 0.31 $\pm$ 0.06              | 0.83 $\pm$ 0.16              | 0.48 $\pm$ 0.11              | 0.90 $\pm$ 0.75  | 1.24 $\pm$ 2.69  |
|     | High-grade     | 0.75 $\pm$ 0.17              | 0.50 $\pm$ 0.11              | 1.00 $\pm$ 0.25              | 0.74 $\pm$ 0.17              | 0.11 $\pm$ 0.43  | -0.11 $\pm$ 1.36 |
|     | <i>F</i> value | 20.894                       | 25.257                       | 6.239                        | 21.068                       | 9.387            | 1.907            |
|     | <i>P</i> value | <0.001**                     | <0.001**                     | 0.017*                       | <0.001**                     | 0.004**          | 0.176            |
| FA  | Low-grade      | 0.15 $\pm$ 0.06              | 0.05 $\pm$ 0.02              | 0.35 $\pm$ 0.14              | 0.14 $\pm$ 0.06              | 0.84 $\pm$ 0.53  | 1.19 $\pm$ 1.73  |
|     | High-grade     | 0.17 $\pm$ 0.05              | 0.06 $\pm$ 0.02              | 0.38 $\pm$ 0.12              | 0.17 $\pm$ 0.05              | 0.65 $\pm$ 0.59  | 0.67 $\pm$ 1.63  |
|     | <i>F</i> value | 1.439                        | 0.682                        | 0.819                        | 1.081                        | 0.512            | 1.932            |
|     | <i>P</i> value | 0.238                        | 0.414                        | 0.372                        | 0.305                        | 0.479            | 0.173            |
| KFA | Low-grade      | 0.34 $\pm$ 0.06              | 0.16 $\pm$ 0.05              | 0.59 $\pm$ 0.07              | 0.34 $\pm$ 0.07              | 0.40 $\pm$ 0.53  | 0.36 $\pm$ 1.21  |
|     | High-grade     | 0.30 $\pm$ 0.08              | 0.14 $\pm$ 0.04              | 0.53 $\pm$ 0.09              | 0.30 $\pm$ 0.08              | 0.43 $\pm$ 0.50  | 0.14 $\pm$ 1.18  |
|     | <i>F</i> value | 0.789                        | 1.758                        | 1.362                        | 0.547                        | 0.001            | 0.017            |
|     | <i>P</i> value | 0.380                        | 0.193                        | 0.251                        | 0.464                        | 0.980            | 0.897            |

Note: a  $\times 10^{-3}$  mm<sup>2</sup>/s \*  $P < 0.05$  \*\*  $P < 0.01$

**Table 2** Logistical regression analysis of mean MK

|          | B     | SE   | Wald | P     |
|----------|-------|------|------|-------|
| Model 1  |       |      |      |       |
| mean MK  | 18.93 | 6.21 | 9.31 | 0.002 |
| Model 2  |       |      |      |       |
| mean MK* | 22.24 | 8.82 | 6.35 | 0.012 |

\*adjusted by age

skewness ADC values increase. In addition, when the data distribution is steeper, the kurtosis ADC values increase.

The FA values in glioma grading showed considerable variations from previously reported findings. Alexiou et al. [3] and Liu et al. [7] showed that the FA values of low-grade gliomas were significantly lower than those of high-grade gliomas, and the FA values of tumours were positively correlated with the Ki-67 index [3]. However, other studies have shown that the FA values were not significantly different between low- and high-grade gliomas and could not be used to distinguish low-grade gliomas from high-grade gliomas [4, 5, 10, 12, 21]. In the present study, the average, minimum, maximum, and median FA values of low-grade gliomas were higher than those of high-grade gliomas, while the kurtosis and skewness FA values were lower, although no significant differences between the groups was observed, consistent with the findings of later studies. The more significant increase in FA values of high-grade gliomas may reflect their more complex histopathological microstructures. The quantity and density of high-grade glioma cells are higher [3, 7]; specifically, glioblastomas often have pseudopalisading and chrysanthemum-like structures, with obvious blood vessels and vascular endothelial hyperplasia and more orderly arranged tumour cells, thereby resulting in increased FA values [24].

DKI can quantify the degree of diffusion restriction or tissue complexity [25], and more complex tissue structures are correlated with higher MK values [8, 18]. Raab et al. [10] showed that the average MK values of grade II astrocytomas, grade III astrocytomas and glioblastomas were  $0.48 \pm 0.02$ ,  $0.62 \pm 0.03$ , and  $0.81 \pm 0.04$ , respectively, and significant differences between two of the groups were observed. Some studies showed that the average MK values were significantly lower in low-grade gliomas than those in high-grade gliomas [5, 12,

21, 26]. In the present study, the mean and median MK values of low-grade gliomas were significantly lower than those in high-grade gliomas, and mean MK was the best independent predictor of differentiating glioma grades ( $B=18.934$ ,  $P=0.002$ ), which may be affected by age because the B value was higher when adjusted by age. Thus, the true efficiency of the mean MK value in differentiating glioma grades might be partially decreased by age. Our findings were consistent with those of previous studies [4, 27, 28], as van Cauter et al. [12] and Falangola et al. [29] found a distinct decrease in mean kurtosis with age. However, high-grade gliomas have more complex tissue structures and higher MK values and are frequently observed in older patients [1]. Those factors may be the main reasons why age could decrease the true efficiency of mean MK in differentiating glioma grades. More complex cell structure, higher cell densities, and more striking nuclear atypia and nuclear pleomorphism, which is associated with greater angiogenesis and tissue necrosis, are observed in high-grade gliomas [10, 12]. Thus, the mean, minimum, maximum, and median MK values of high-grade gliomas were higher than those of low-grade gliomas. Gliomas are frequently observed in white matter, and previous studies [5, 10, 12] have shown that the MK values increase with increasing glioma grade but remain lower than those of normal white matter. In other words, the complexity of the glioma structure increases with increasing glioma grade, and the MK value is closer to that of normal white matter; thus, the histogram distribution of the MK values of high-grade gliomas is skewed to the right, with skewness closer to 0 (skewness of normal distribution is 0).

KFA is mathematically analogous to FA and represents a parameter of kurtosis tensor and an extension of fractional anisotropy in kurtosis tensor. Similar to FA, lower KFA values are correlated with higher isotropic diffusion. Previous studies have shown that KFA provides additional diffusion information and can better assess the complexity of tissue structures [30, 31]. KFA is currently not used for glioma grading. In the present study, the histogram parameters of KFA were not significantly different between high- and low-grade gliomas, which was similar to the results of a previous report by Stadlbauer et al. [32]. In addition, the KFA value of the solid regions of gliomas was significantly higher than the FA value, which is consistent with the results obtained from the analysis brains from healthy volunteer and rats [30, 31]. We also

**Table 3** ROC results of partial DKI metrics histogram parameters

| Diagnostic index | AUC   | Cutoff value | Se (%)       | Sp (%)        | PPV (%)       | NPV (%)      | Accuracy (%) |
|------------------|-------|--------------|--------------|---------------|---------------|--------------|--------------|
| MD_mean          | 0.870 | 1.29         | 92.3 (12/13) | 65.4 (17/26)  | 57.1 (12/21)  | 94.4 (17/18) | 74.4 (29/39) |
| MD_min           | 0.796 | 0.94         | 92.3 (12/13) | 65.4 (17/26)  | 57.1 (12/21)  | 94.4 (17/18) | 74.4 (29/39) |
| MK_mean          | 0.925 | 0.63         | 88.5 (23/26) | 84.6 (11/13)  | 92.0 (23/25)  | 78.6 (11/14) | 87.2 (34/39) |
| MK_min           | 0.926 | 0.42         | 84.6 (22/26) | 100.0 (13/13) | 100.0 (22/22) | 76.5 (13/17) | 89.7 (35/39) |

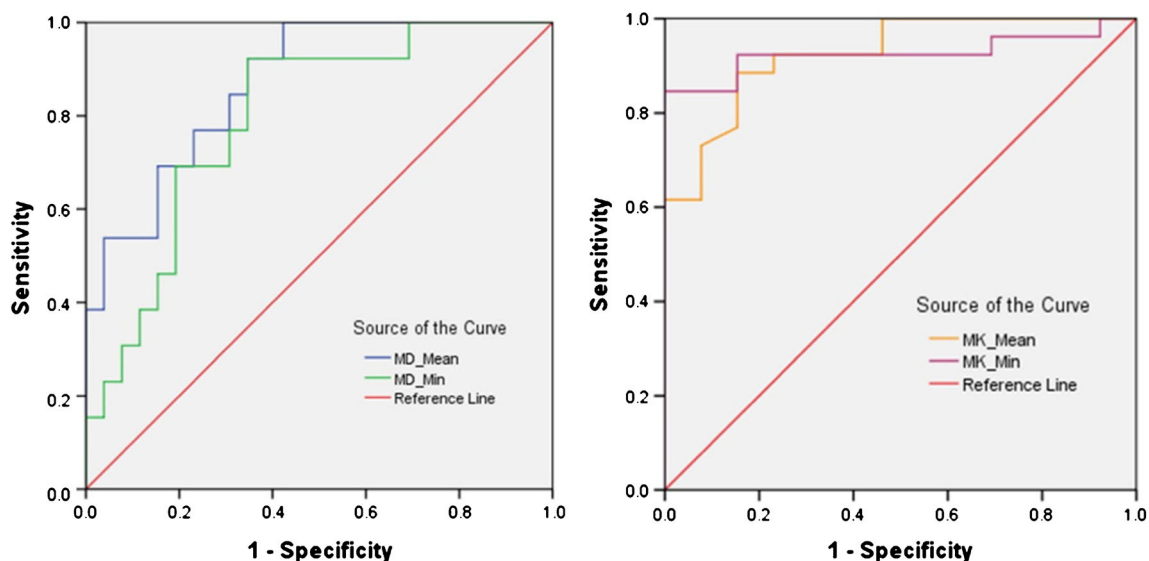


**Fig. 3** ROC curve of partial DKI metrics histogram parameters in differentiating low- and high-grade gliomas

observed a positive correlation between FA and KFA, with a partial correlation coefficient of 0.675 ( $P < 0.001$ ). The KFA value of high-grade gliomas was lower than that of low-grade gliomas, while the opposite was observed for FA (the FA value of high-grade gliomas was higher than that of low-grade gliomas). Thus, these results require further study.

Previous studies [12, 29] have shown that the diagnostic efficiency of MD, MK, and FA may be affected by age. In the present study, the age span of the patient group with high-grade gliomas was larger than that of the low-grade glioma group. Hence, to eliminate age-related influences on parameter estimation, we also used a univariate linear modelling analysis that included age as a covariate to test the differences of mean DKI parameters between glioma grades, which made the parameters dependent on tissue properties related to the disease and not age. We found significant differences in the abilities of mean MD and mean MK to differentiate glioma grades ( $F = 19.127$ ,  $P < 0.001$  and  $F = 20.894$ ,  $P < 0.001$ , respectively), which is consistent with the results of previous studies.

Tietze et al. [26] reported the higher diagnostic value of MK and MD when optimum diagnostic thresholds of MK and MD were 0.58 and  $1.46 \times 10^{-3} \text{ mm}^2/\text{s}$ , respectively. The results of the present study are consistent with those of previous studies. We observed the AUC and cut-off value of the mean MD to be 0.870 and  $1.29 \times 10^{-3} \text{ mm}^2/\text{s}$ , respectively, and the sensitivity, specificity and accuracy were 92.3%, 65.4%, and 74.4%, respectively. The AUC and cut-off value of the mean MK were 0.925 and 0.63, respectively, and the sensitivity, specificity, and accuracy were 88.5%, 84.6%, and 87.2%, respectively. The specificity and accuracy of the mean MK were higher than those of the mean MD [5, 27]. In addition, the minimum MK values showed high diagnostic efficiency, which was close to those of mean MK.

The present study also had some limitations. Although we optimised the DKI scanning protocol based on previous studies, the scan time and data post-processing time were still relatively long. Tietze et al. [26] proposed a new and faster DKI method, with scanning and data post-processing times of 166 s and 3–5 s, enabling larger-scale implementation in clinical studies. Furthermore, the number of low-grade glioma patients was relatively small, and the reliability of the results should be confirmed in larger patient samples by prospective studies.

In conclusion, the present study demonstrated significant differences in the DKI parameters between high- and low-grade gliomas using the histogram analysis of DKI-derived maps. Mean MK was the best independent predictor of differentiating glioma grades.

**Funding** This study has received funding by National Natural Science Foundation of China (No. 81101035).

**Compliance with ethical standards**

**Guarantor** The scientific guarantor of this publication is Xu Ke.

**Conflict of interest** The authors of this manuscript declare no relationships with any companies, whose products or services may be related to the subject matter of the article.

**Statistics and biometry** No complex statistical methods were necessary for this paper.

**Informed consent** Written informed consent was not required for this study because all patients had signed the hospitalised informed consents.

**Ethical approval** Institutional Review Board approval was not required because the study does not involve ethical issues.

**Methodology**

- retrospective
- diagnostic or prognostic study
- performed at one institution

**References**

- Ostrom QT, Gittleman H, Liao P et al (2014) CBTRUS statistical report: primary brain and central nervous system tumors diagnosed in the United States in 2007–2011. *Neuro Oncol* 16:iv1–iv63
- Louis DN, Perry A, Reifenberger G et al (2016) The 2016 world health organization classification of tumors of the central nervous system: a summary. *Acta Neuropathol* 131:803–820
- Alexiou GA, Zikou A, Tsiouris S et al (2014) Correlation of diffusion tensor, dynamic susceptibility contrast MRI and (99m)Tc-Tetrofosmin brain SPECT with tumour grade and Ki-67 immunohistochemistry in glioma. *Clin Neurol Neurosurg* 116:41–45
- Jakab A, Molnár P, Emri M, Berényi E (2011) Glioma grade assessment by using histogram analysis of diffusion tensor imaging-derived maps. *Neuroradiology* 53:483–491
- Jiang R, Jiang J, Zhao L et al (2015) Diffusion kurtosis imaging can efficiently assess the glioma grade and cellular proliferation. *Oncotarget* 6:42380–42393
- Xiao HF, Chen ZY, Lou X et al (2015) Astrocytic tumour grading: a comparative study of three-dimensional pseudocontinuous arterial spin labelling, dynamic susceptibility contrast-enhanced perfusion-weighted imaging, and diffusion-weighted imaging. *Eur Radiol* 25:3423–3430
- Liu X, Tian W, Kolar B et al (2011) MR diffusion tensor and perfusion-weighted imaging in preoperative grading of supratentorial nonenhancing gliomas. *Neuro Oncol* 13:447–455
- Jensen JH, Helpem JA (2010) MRI quantification of non-Gaussian water diffusion by kurtosis analysis. *Biomedicine* 23:698–710
- Tabesh A, Jensen JH, Ardekani BA, Helpem JA (2011) Estimation of tensors and tensor-derived measures in diffusional kurtosis imaging. *Magn Reson Med* 65:823–836
- Raab P, Hattingen E, Franz K, Zanella FE, Lanfermann H (2010) Cerebral gliomas: diffusional kurtosis imaging analysis of microstructural differences. *Radiology* 254:876–881
- Hui ES, Cheung MM, Qi L et al (2008) Towards better MR characterization of neural tissues using directional diffusion kurtosis analysis. *NeuroImage* 42:122–134
- van Cauter S, Veraart J, Sijbers J et al (2012) Gliomas: diffusion kurtosis MR imaging in grading. *Radiology* 263:492–501
- Just N (2014) Improving tumour heterogeneity MRI assessment with histograms. *Br J Cancer* 111:2205–2213
- Kyriazi S, Collins DJ, Messiou C et al (2011) Metastatic ovarian and primary peritoneal cancer: assessing chemotherapy response with diffusion-weighted MR imaging—value of histogram analysis of apparent diffusion coefficients. *Radiology* 261:182–192
- Suo S, Zhang K, Cao M et al (2016) Characterization of breast masses as benign or malignant at 3.0T MRI with whole-lesion histogram analysis of the apparent diffusion coefficient. *J Magn Reson Imaging* 43:894–902
- Wang S, Kim S, Zhang Y et al (2012) Determination of grade and subtype of meningiomas by using histogram analysis of diffusion-tensor imaging metrics. *Radiology* 262:584–592
- Xu XQ, Hu H, Su GY et al (2016) Utility of histogram analysis of ADC maps for differentiating orbital tumors. *Diagn Interv Radiol* 22:161–167
- Jensen JH, Falangola MF, Hu C et al (2011) Preliminary observations of increased diffusional kurtosis in human brain following recent cerebral infarction. *Biomedicine* 24:452–457
- Lee J, Choi SH, Kim JH et al (2014) Glioma grading using apparent diffusion coefficient map: application of histogram analysis based on automatic segmentation. *NMR Biomed* 27:1046–105220
- Arevalo-Perez J, Peck KK, Young RJ et al (2015) Dynamic contrast-enhanced perfusion MRI and diffusion-weighted imaging in grading of gliomas. *J Neuroimaging* 25:792–798
- van Cauter S, de Keyser F, Sima DM et al (2014) Integrating diffusion kurtosis imaging, dynamic susceptibility-weighted contrast-enhanced MRI, and short echo time chemical shift imaging for grading gliomas. *Neuro-Oncology* 16:1010–1021
- Chen SD, Hou PF, Lou L, Jin X, Wang TH, Xu JL (2014) The correlation between MR diffusion-weighted imaging and pathological grades on glioma. *Eur Rev Med Pharmacol Sci* 18:1904–1909
- Kang Y, Choi SH, Kim YJ et al (2011) Gliomas: Histogram analysis of apparent diffusion coefficient maps with standard- or high-b-value diffusion-weighted MR imaging—correlation with tumor grade. *Radiology* 261:882–890
- Beppu T, Inoue T, Shibata Y et al (2003) Measurement of fractional anisotropy using diffusion tensor MRI in supratentorial astrocytic tumors. *J Neuro-Oncol* 63:109–116
- Wu EX, Cheung MM (2010) MR diffusion kurtosis imaging for neural tissue characterization. *NMR Biomed* 23:836–848
- Tietze A, Hansen MB, Østergaard L et al (2015) Mean diffusional kurtosis in patients with glioma: initial results with a fast imaging method in a clinical setting. *Am J Neuroradiol* 36:1472–1478
- Bai Y, Lin Y, Tian J et al (2016) Grading of gliomas by using monoexponential, biexponential, and stretched exponential diffusion-weighted MR imaging and diffusion kurtosis MR imaging. *Radiology* 278:496–504
- Qi C, Yang S, Meng L et al (2017) Evaluation of cerebral glioma using 3T diffusion kurtosis tensor imaging and the relationship between diffusion kurtosis metrics and tumor cellularity. *J Int Med Res* 45:1347–1358
- Falangola MF, Jensen JH, Babb JS et al (2008) Age-related non-Gaussian diffusion patterns in the prefrontal brain. *J Magn Reson Imaging* 28:1345–1350
- Glenn GR, Helpem JA, Tabesh A, Jensen JH (2015) Quantitative assessment of diffusional kurtosis anisotropy. *Biomedicine* 28:448–459
- Hansen B, Jespersen SN (2016) Kurtosis fractional anisotropy, its contrast and estimation by proxy. *Sci Rep* 6:23999
- Stadlbauer A, Ganslandt O, Buslei R et al (2006) Gliomas: histopathologic evaluation of changes in directionality and magnitude of water diffusion at diffusion-tensor MR imaging. *Radiology* 240:803–810